14th WEGEMT, Trondheim Norway, 21st – 25th of January 1991

Pipeline Stresses and Deformations During Laying

by

Preben Terndrup Pedersen

Department of Ocean Engineering
The Technical University of Denmark
DK–2800 Lyngby, Denmark

1. Introduction

With increasing water depth the length of the suspended pipeline between the pipelaying barge and the ocean floor becomes greater. This may cause the stresses in the pipe to become so high that the pipe buckles or the stresses in the stinger to reach a level where the stinger is damaged. The engineering design of marine pipeline systems raises the problem of static and dynamic analysis of pipelines. Therefore, analysis tools are needed which can accurately predict the static equilibrium curve and the dynamic response characteristics of pipelines. With such tools one can establish the limits for water depths and environmental conditions in which the pipe can be layed or lay the pipe along a desired path.

Marine pipelines can be modelled as beams rather than shells because their diameter–to–length ratios are small.

The problem of predicting the suspended geometry and thereby the stress of marine pipelines during laying in the ocean is one of large deflection beam theory, where the length of the suspended beam is not a priori known.

There is a vast and steadily growing literature on pipeline problems. Here we shall cite only a limited number of important papers where reference to earlier work may be found.

Let us first consider research devoted to the two–dimensional problem of analysing a plane pipeline subjected to static loads in the plane of bending during normal laying.

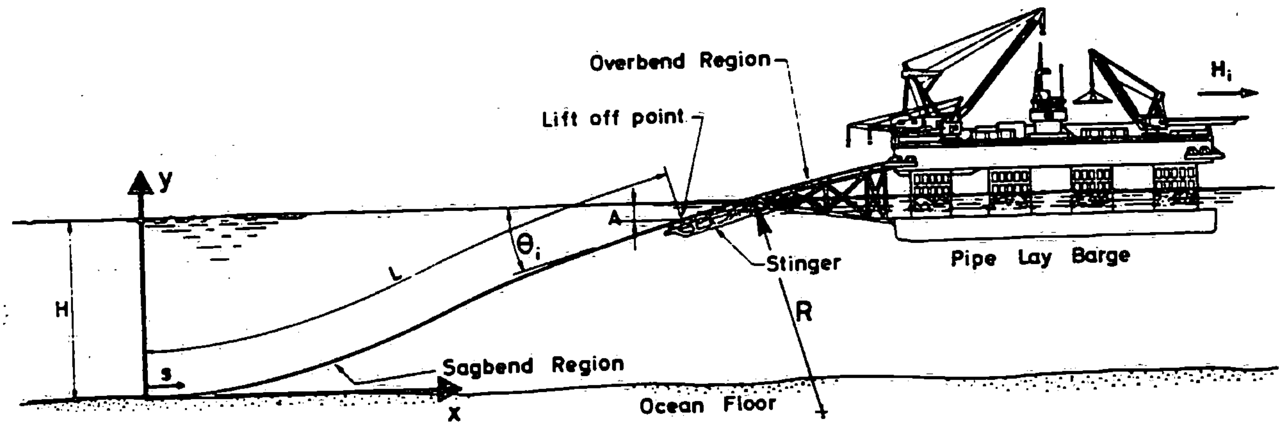

Fig. 1.1. Conventional pipelaying

R. Plunkett [1] and D.A. Dixon and D.R. Rutledge [2] used the stiffened catenary method to get solutions, which are based on the assumption that the pipeline takes a shape which can be approximated as a natural catenary over most of its length and where the influence of the boundary conditions is confined to small "boundary layers" near the end supports. The main advantage of this method is relatively small demands on numerical calculations. But it is only valid in such cases where the tension rather than the bending stiffness governs the behaviour over most of the length, that is the pipeline has a relatively small bending stiffness or is to be placed in deep water. It is usually not flexible enough to handle all the existing types of pipelaying procedures.

J.T. Powers and L.D Finn [3] solve the 2–D problem through the use of a finite element method and an initial–value approach. They treat the pipeline as a series of small beams each of which are treated as linear elements. This method possesses several advantages due to the fact that any desired boundary condition, in principle, can be considered and the beam properties and loads can be varied from element to element. But the primary limitation of this method is its loss of accuracy and failure to converge for pipelines layed in deep water or with small stiffness. Furthermore, the boundary conditions must be satisfied from one end to another by a trial and error procedure using an initial–value approach. It needs laborious computations even for 2–D analyses.

A.C. Palmer et al. [4] and D.W. Darling and R.F. Neathery [5] derive differential equations governing the equilibrium configuration of the plane pipe. The result is a non–linear two–point boundary value problem. A finite–difference solution procedure is described in these papers. In [5], the series truncation is used to linearize the governing equations. In [4] the nonlinear differential equations are transformed into a non–dimensional form and a non–dimensionlised suspended length is introduced. The resulting equations together with end conditions are expressed as a set of simultaneous linear algebraic equations by moving nonlinear terms to the right hand sides of the equations. Then successive iterations are used to get numerical solutions. This latter method seems better than the initial value approach because less programming effort is needed and the difficulties with instability are reduced. Common to these methods is that each main iteration step involves a second set of successive iterations for the calculation of the suspended length. This fact causes a relatively large demand to computer size and time.

P. Terndrup Pedersen [6] presents a relatively direct solution method to cable and pipelaying problems. The governing nonlinear two–point boundary value problem is derived and transformed into a non–dimensional form such that the a priori unknown suspended length of the pipeline acts as a scaling parameter. The method of solution is then based on successive integrations. This method possesses the principal advantage, that it has extremely modest requirements to computer storage and computer time because the solution only involves integration of known functions and only one set of successive iterations is needed. Another advantage is its flexibility to model different types of pipelaying procedures. Through a modification [7], this method has been improved so that it is also an efficient solution technique for pipelines with large or very small bending stiffnesses and for laying procedures in shallow or very deep water.

The most accurate prediction of stresses and trajections of pipelines during laying is achieved by three–dimensional analysis. This is due to the fact that the various laying procedures and the external loads due to current, wave and wind in different angles to the direction of laying deflect the pipelines in the shape of 3–D curves. Furthermore, close to platforms where many obstacles and existing pipelines may be present it is often necessary to lay pipes in curved trajections with great precision. Therefore, in recent years some attempts have been made to solve 3–D problems.

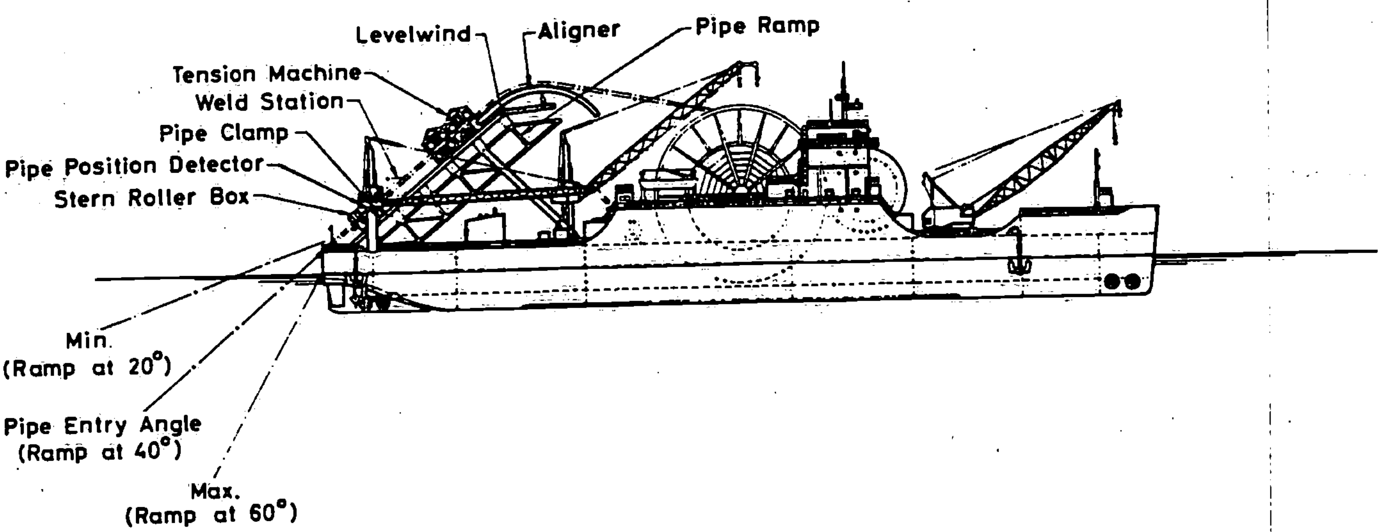

Fig. 1.2. The dynamically positioned reel ship APACHE is designed to spool and lay pipe up to 16 inches in diameter.

T.N. Gardner et al. [8] developed a 3–D analysis technique for risers in deep water using FEM. They employed "small angle, large deflection" assumptions so that the terms coupling torsion and transverse bending and the terms coupling the displacements in the direction of the two principal axes of the cross–section can be considered insignificant. The Newmark method with inclusion of an iterative relaxation is used for the numerical calculations.

J.S. Chung and C.A. Felippa [9] present a nonlinear 3–D static analysis procedure for deep ocean mining pipes or risers. The finite–element technique is also used in their paper, where the pipeline – with a known length – is modeled by 3–D nonlinear beam elements. The deformations due to tension, bending or torsion are included. The modified Newton iteration method is used to get a solution. The FEM has the flexibility to model variations of external loads or cross–sectional properties along the pipe length together with any desired boundary condition. But it seems that much more effort will be needed to get precise and convergent solution in the case of pipelines with unknown lengths or in deep water.

M.M. Bernitsas [10], and M.B. Bryndum et al. [11] have developed the 3–D nonlinear model for large–deflection behaviour of pipelines using a local orthogonal coordinate system. In [11], the resulting differential eqs. have been solved numerically by a finite difference approximation. Common to the models in [10] and [11] is that the local moving coordinate systems are defined only by the central–line. This results in the inherent limitation that the numerical solutions based on such models can only describe the deformations of the central–line and the torsional deformation of the pipe cross–sections cannot be taken into account.

R.P. Nordgren [12], [13] sets up the 3–D large deflection non–linear model in the local principal system by vector analysis, where the torsional moment in stead of torsional deformation appears in the governing equations. This model can only be used to describe the behaviour of pipelines with equal principal stiffnesses and the torsional moment at one of the two ends should be known in advance. The torsional deformation cannot be described.

Also Molahy [14] has presented a 3–D finite element procedure which can be used to study the geometrical non–linear equilibrium curves.

Based on a finite difference procedure Yan Junqi and P. Terndrup Pedersen [15] and [16] have developed a consistent non–linear model for 3–D large deflection analysis of pipelines within the small strain beam theory. This model can take into account all the non–linearities due to geometry, arbitrary variation of loads, different boundary conditions and variation of the pipe properties. It can be used to describe not only the behaviour of pipes with symmetric cross–sections but also of pipes with asymmetric cross–sections such as piggy backed pipelines. The often used approximations leading to the inconsistent equilibrium equation are avoided, and the procedure makes it possible to describe the torsional deformations of the pipeline.

In the following we shall present a method for 2–D analysis based on Refs. [6] and [7] which provides a relatively direct solution pipe–laying problems. The governing non–linear, two–point boundary value problem is derived and transformed into a non–dimensional form such that the a priori unknown suspended length of the pipeline or cable acts as a scaling parameter.

2. Loading on the suspended pipe

We consider a deformed inextensible pipe as shown in Figure 2.1. As independent variable in our formulation we shall employ the arc length s from the point where the pipe touches the ocean floor. This point will also serve as origin for the rectangular coordinate system X–Y shown in Figure 2.1. The tangent angle to the pipe is denoted $\theta(s)$, and we designate the depth of the ocean by H.

The load on an element of unit length of the suspended pipe is composed of: the weight $w_t(s)$, the buoyancy $w_0(s)$ and, due to a steady ocean current with velocity V(Y), also a normal drag force $F_n(s)$ and a tangential drag force $F_t(s)$.

The mass density of the water is given by ρ_V, the gravity by g, and the cross sectional area of the pipe by a.

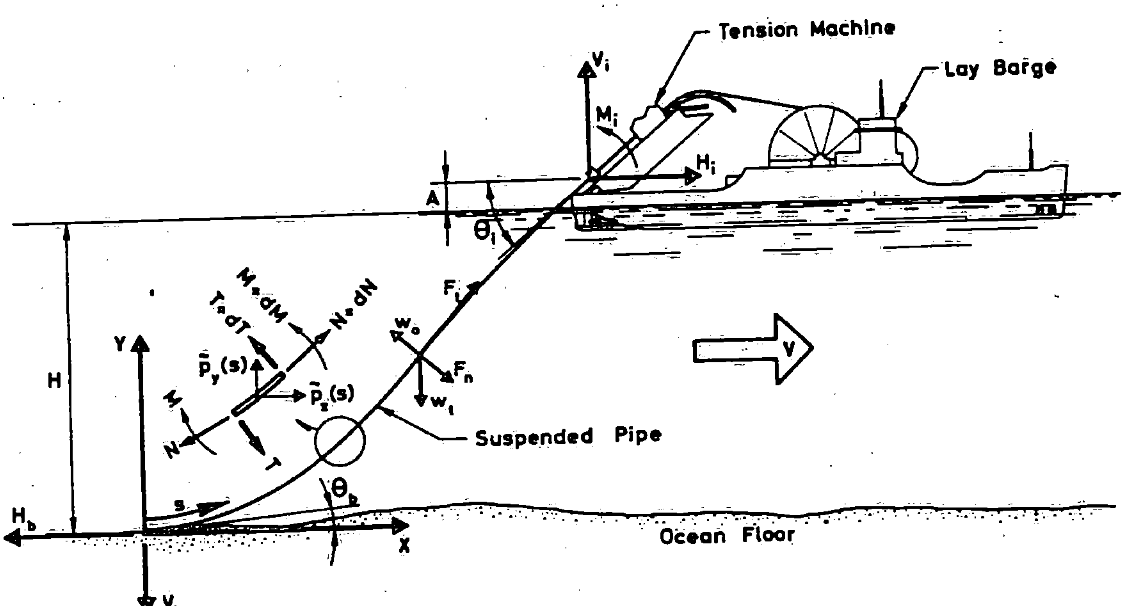

Figure 2.1. Loading on the pipe

The buoyancy load on the pipe due to the water pressure is determined as follows. Consider the segment of length ds shown in Figure 2.2. The total buoyancy of the segment with "open ends" equals $\rho_V$ga ds and acts in the Y–direction. This load has to be corrected for the lack of pressure at the ends of the segment. From Figure 2.2 it follows that the resulting buoyancy load $w_0$ds acts in the direction normal to the centerline of the pipe segment and

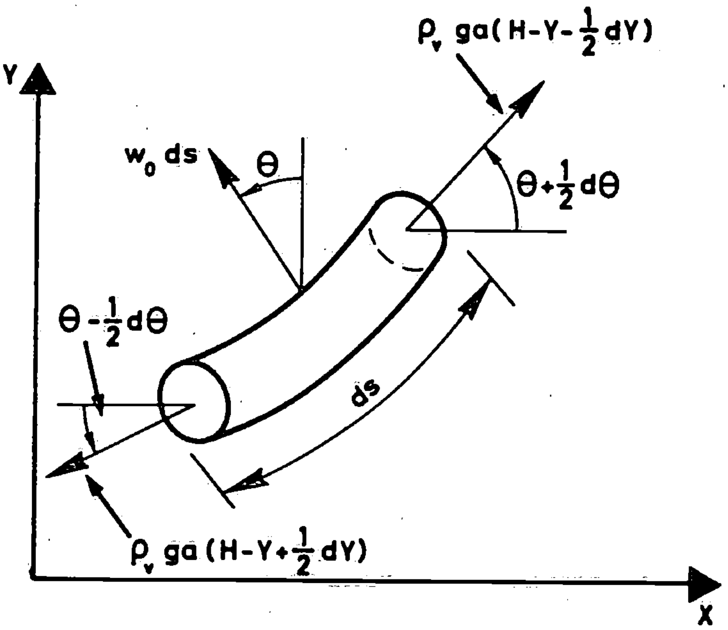

Figure 2.2. Buoyancy on pipe element.

with a magnitude given by

$$w_0 = w_b \left\{\cos\theta + (H - Y)\,\frac{d\theta}{ds}\right\} \tag{2.1}$$

where $w_b = \rho_v\, ga$ for $0 \leq Y \leq H$ and $w_b = 0$ for $Y > H$.

The loading due to the current takes the form

$$F = \frac{1}{2}\,\rho_v\, C|V|\, V\, A_c \tag{2.2}$$

where C is the drag coefficient, V the flow velocity, and A_c a characteristic area. The axial and tangential load per unit length can be obtained from (2.2) as

$$\begin{aligned} F_n &= \frac{1}{2}\,\rho_v\, C_n\, V|V|D\, \sin^2\theta \\ F_t &= \frac{1}{2}\,\pi\,\rho_v\, C_t\, V|V|D\, \cos^2\theta \end{aligned} \tag{2.3}$$

where D is the diameter of the pipe, and C_n, C_t are drag coefficients.

Thus, the resulting horizontal and vertical load intensities for the submerged part of the pipe are

$$\tilde{p}_x(s) = F_t \cos\theta - \left[w_0 - F_n\right]\sin\theta$$
$$\tilde{p}_y(s) = F_t \sin\theta + \left[w_0 - F_n\right]\cos\theta - w_t \tag{2.4}$$

respectively.

3. Governing equations for the pipeline

In this section we shall set up the governing equations for the plane, one–dimensional, finite strain beam theory which will be used to model the pipe.

As constitutive law for the pipe we will assume a linear relation between the bending moment M and the curvature $d\theta/ds$. Thus

$$M(s) = EI \frac{d\theta}{ds} \tag{3.1}$$

where EI is the bending stiffness of the pipe.

The moment equilibrium condition for segments of the pipe give the shear force T(s) as

$$T(s) = -\frac{dM}{ds} = -\frac{d}{ds} EI\left[\frac{d\theta}{ds}\right] \tag{3.2}$$

The shear force T at any section of the pipe can be found from Figure 2.1 by equilibrium considerations. We find

$$T(s) = -\frac{d}{ds}\left[EI \frac{d\theta}{ds}\right]$$
$$= H_b \sin\theta(s) + V_b \cos\theta(s) - \cos(s) \int_0^s \tilde{p}_y(s_1)ds_1$$
$$+ \sin\theta(s) \int_0^s \tilde{p}_x(s_1)ds_1 \tag{3.3}$$

where H_b, V_b are the horizontal and vertical force components, respectively, at the support point at the ocean floor. Similarly, we find the axial force N(s) at any section of the suspended pipe as

$$
\begin{aligned}
N(s) \quad &= H_b \cos\theta(s) + V_b \sin\theta(s) - \sin\theta(s) \int_0^s p_y(s_1) ds_1 \\
&- \cos\theta(s) \int_0^s \tilde{p}_x(s_1)\, ds_1
\end{aligned}
\tag{3.4}
$$

The equations (3.3) and (3.4) can also be written in the form

$$
\begin{aligned}
\frac{d}{ds}\left[EI \frac{d\theta}{ds}\right] \quad &= \hat{H}_b \sin\theta(s) - \hat{V}_b \cos\theta(s) + \cos\theta(s) \int_0^s \hat{p}_y(s_1) ds_1 \\
&- \sin\theta(s) \int_0^s \hat{p}_x(s_1) ds_1
\end{aligned}
\tag{3.5}
$$

and

$$
\begin{aligned}
\hat{N}(s) \quad &= \hat{H}_b \cos\theta(s) - \hat{V}_b \sin\theta(s) - \sin\theta(s) \int_0^s \hat{p}_y(s_1) ds_1 \\
&- \cos\theta(s) \int_0^s \hat{p}_x(s_1) ds_1
\end{aligned}
\tag{3.6}
$$

where

$$\hat{p}_y(s) \quad = F_t \sin\theta(s) - F_n \cos\theta(s) - \left[w_t - w_b\right]$$

$$\hat{p}_x(x) \quad = F_t \cos\theta(s) + F_n \sin\theta(s)$$

$$\hat{H}_b \quad = H_b + Hw_b \cos\theta_v \quad ; \quad \hat{V}_b = V_b + Hw_b \sin\theta_b$$

and

$$\hat{N} \quad = N + \{H - Y(\bar{s})\} w_b$$

Equation (3.5) shows that the effect of the buoyancy on the equilibrium curve of the pipe can be accounted for by introducing the submerged weight of the pipe. However, it will be seen from equation (3.6) that taking care of the buoyancy simply by introducing the submerged weight results in an apparent axial force $\hat{N}$ which equals the real axial force N plus the hydrostatic force $w_b(H - Y)$. Here, we may note that for the evaluation of the buckling strength of a pipe it is the real axial force N that is of importance, whereas for the determination of a reference stress for a solid cable or mooring line we will be concerned with the adjusted axial force which here is denoted $\hat{N}$.

In order to isolate the unknown suspended length L of the pipe let us then introduce the following dimensionless quantities:

$$\xi = s/L \quad ; \quad \{x,y\} = \{X,Y\}/L \quad ; \quad \lambda = L/H$$

$$\gamma = \frac{EI}{w_t^0 H^3} \quad ; \quad \left\{p_x, p_y\right\} = \left\{\hat{p}_x, \hat{p}_y\right\}/w_t^0$$

and

$$\left\{h_b, v_b, n, t\right\} = \left\{\hat{H}_b, \hat{V}_b, \hat{N}, T\right\}/\left[w_t^0 H\right]$$

where w_t^0 is a characteristic value of the weight per unit length w_t of the pipe. Then equation (3.5) takes the form

$$\lambda^{-2} \frac{d}{d\xi}\left[\gamma \frac{d\theta}{d\xi}\right] = h_b \sin\theta - v_b \cos\theta$$

$$+ \lambda \left\{\cos\theta \int_0^\xi p_y \, d\xi_1 - \sin\theta \int_0^\xi p_x \, d\xi_1\right\} \qquad (3.7a)$$

and equation (3.6) takes the form

$$n(\xi) = h_b \cos\theta + v_b \sin\theta$$

$$- \lambda \left\{ \sin\theta \int_0^{\xi} p_y \, d\xi_1 + \cos\theta \int_0^{\xi} p_x \, d\xi_1 \right\} \tag{3.7b}$$

By differentiation of Eq. (3.7a) and use of Eq. (3.7b) we obtain

$$\frac{d^2}{d\xi^2} \left[\gamma \frac{d\theta}{d\xi} \right] - \lambda^2 \, n(\xi,\theta) \frac{d\theta}{d\xi} = \lambda^3 \cdot p(\xi,\theta) \tag{3.8}$$

where

$$p(\xi,\theta) = \cos\theta(\xi) \cdot p_y(\xi) - \sin\theta(\xi) \, p_x(\xi)$$

Neglecting the axial extension of the pipe, the relation between the dimensionless natural coordinates (θ,ξ) and the dimensionless rectangular coordinates (x,y) are

$$dy = \sin\theta \, d\xi \quad \text{and} \quad dx = \cos\theta \, d\xi \tag{3.9}$$

The boundary conditions at the ocean floor are taken as:

$$y(0) = x(0) = 0 \tag{3.10}$$

$$\theta(0) = \theta_b \tag{3.11}$$

$$\left[\frac{d\theta}{\partial\xi}\right]_{\xi=0} = 0 \tag{3.12}$$

The boundary conditions at the upper end of the suspended pipe depend on the method of operation (for example the type of stinger used). But we note, for future use, that the dimensionless applied horizontal tension can be found from the following equilibrium equation

$$h_i = h_b - \lambda \int_0^1 p_x \, d\xi_1 \tag{3.13}$$

and that the vertical component of the tension is given by

$$v_i = v_b - \lambda \int_0^1 p_y \, d\xi_1 \tag{3.14}$$

Here the non–dimensional forces h_i, v_i are related to the applied forces H_i, V_i by

$$h_i = \left\{H_i + \left[H - Y_i\right] w_b \cos\theta_i\right\} / \left[w_t^0 \, H\right]$$

and

$$v_i = \left\{V_i + \left[H - Y_i\right] w_b \sin\theta_1\right\} / \left[w_t^0 \, H\right]$$

The differential equations (3.8) and (3.9) and the boundary conditions of the problem constitute the non–linear boundary value problem to be solved.

4. Solution Procedure

A. Pipe–laying without stinger or with an articulated stinger

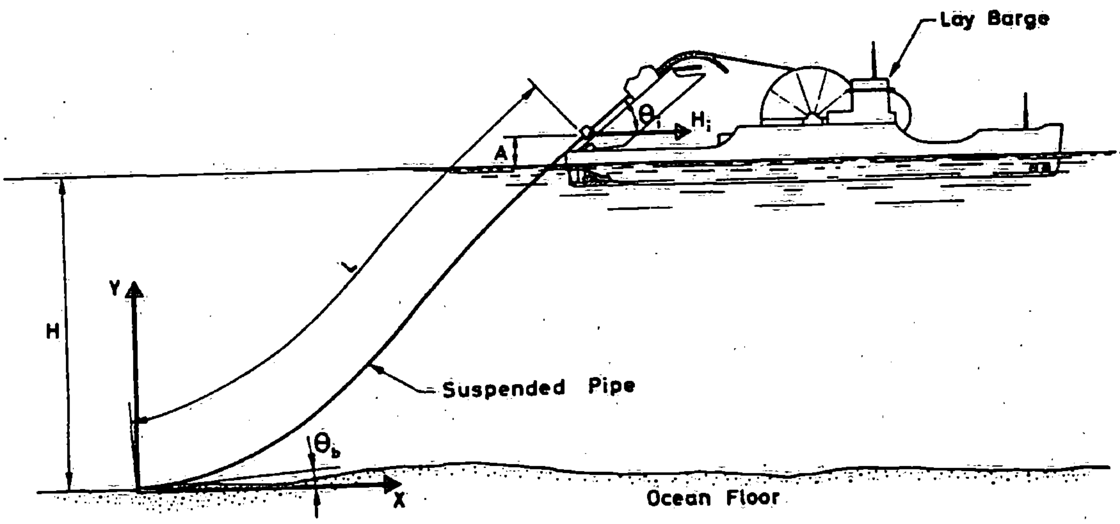

Figure 4.1. Pipe–laying without stinger.

First we shall consider a case where the pipe is layed without the use of a stinger. See Fig. 4.1. We shall assume that at the upper end of the suspended pipe we have the kinematic boundary conditions

$$\theta(L) = \theta_i \tag{4.1}$$

$$Y(L) = H + A \tag{4.2}$$

where A is the distance between the pipe support on the barge and the ocean surface. We shall also assume that the applied horizontal tension H_i at the support is known.

In order to solve this non–linear boundary value problem we shall assume that the loading $p_j\left[\xi,\theta_j\right]$ and the axial tension $n_j\left[\xi,\theta_j\right]$ associated with an arbitraty deflection curve $\left\{\theta_j,\ x_j,\ y_j,\ \lambda_j\right\}$ is determined. Then a new improved solution vector $\left\{\theta_{j+1},\ x_{j+1},\ y_{j+1},\ \lambda_{j+1}\right\}$ can be found in the following way.

First the dimensionless moment distribution $m_j(\xi) = \gamma \dfrac{d\theta_j}{d\xi}$ is introduced and an algorithm based on equation (3.8) is obtained in the form

$$\frac{d^2}{d\xi^2}\left\{m_{j+1}(\xi)\right\} - \lambda_j^2 \frac{n_j(\xi)}{\gamma(\xi)} m_{j+1}(\xi) = \lambda_{j+1}^{\alpha} \left\{\lambda_j^{3-\alpha}\ p_j(\xi)\right\} \tag{4.3}$$

Here the exponent α is chosen such that fast convergence is obtained. It can be shown that this choice must depend on the value of $r = L\left[\dfrac{H_i}{EI}\right]^{1/2}$. However in most realistic pipe–laying problems $\alpha = 3$ is a good choice.

From equation (4.3) an improved moment distribution $m_{j+1}(\xi)$ can be determined numerically by transforming the equation into finite difference form and solving the resulting linear algebraic system of equations, which has a convenient tri–diagonal form, by Gaussion elimination. This leads to

$$\frac{d\theta_{j+1}}{d\xi} = \frac{m_{j+1}(\xi)}{\gamma(\xi)} = \frac{\lambda_{j+1}^{\alpha}}{\gamma(\xi)}\left\{m_{j+1}^{(1)}(\xi) + m_{j+1}(l)\cdot m_{j+1}^{(2)}(\xi)\right\} \tag{4.4}$$

where $m_{j+1}(l)$ is the so far unknown moment at the upper end of the pipe.

By integration of equation (4.4) and use of the boundary condition $\theta_{j+1}(l) = \theta_i$ to determine $m_{j+1}(l)$ we find

$$\theta_{j+1}(\xi) \quad = \lambda^{\alpha}_{j+1} \cdot g_1(\xi) + g_2(\xi) \tag{4.5}$$

where $g_1(\xi)$ and $g_2(\xi)$ are known functions.

The improved cartesian coordinates to the equilibrium curve are given by

$$x_{j+1}(\xi) \quad = \int_0^{\xi} \cos\theta_{j+1} \; d\xi$$

and (4.6a and b)

$$y_{j+1}(\xi) \quad = \int_0^{\xi} \sin\theta_{j+1} \; d\xi$$

The as yet unknown suspended length of the pipe can now be determined by solving the transcendental equation obtained from the boundary condition $Y(L) = H + A$ and (4.6b):

$$\lambda_{j+1} \quad \cdot \int_0^{l} \sin\left[\lambda^{\alpha}_{j+1} \, g_1(\xi) + g_2(\xi)\right] d\xi$$

$$= 1 + a, \qquad \text{where } a = A/H \tag{4.7}$$

Thus, starting with an arbitrary integrable approximation to the equilibrium curve the functions g_1 and g_2 can be determined from (4.4) and a new approximation to the suspended length of the pipe λ_{j+1} can be found from (4.7). The improved approximation to the equilibrium functions are then found from (4.5), (4.6a) and (4.6b).

The sequence of successive iterations may be started with an arbitrary regular function satisfying the kinematic boundary conditions.

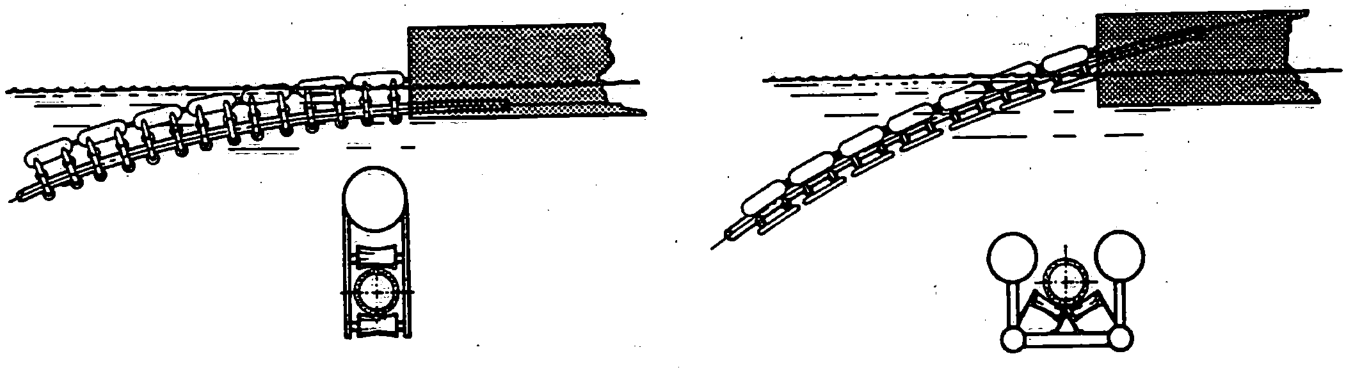

Fig. 4.2. Articulated Stingers.

We can, for example, use the deflection curve corresponding to a natural catenary or a solution of the linearized Bernoulli–Euler beam equation that satisfies all the boundary conditions at the ocean floor and the kinematic boundary conditions at the upper end of the suspended pipe. These methods of obtaining the first approximation also supply us with a first estimate of the suspended length.

The effect of having part of the equilibrium curve above the surface of the ocean ($A > 0$), or support buoys along the pipe, or, an articulated stinger, see Fig. 4.2, is easily taken care of in the present formulation by introducing a variation in the distributed buoyancy and/or weight of the pipe.

As an application of the foregoing, figure 4.3, shows the results of the numerical analysis of a pipe–laying procedure where the pipe is laid without the use of a stinger. The water depth H is 50 m, the pipe leaves the pipe–laying barge 2 m above the water surface at an angle equal to 20^0. The horizontal tension H_i applied at the barge is $2.200 \cdot 10^5$ N. The uniform bending stiffness EI of the pipe is $2.256 \cdot 10^9$ Nm^2, the buoyancy per unit length in water w_b is $1.614 \cdot 10^4$ N/m and the weight per unit length w_t is $1.843 \cdot 10^4$ N/m.

Starting with a deflection curve corresponding to the solution of the linearized beam equation, where the effect of the applied horizontal tension H_i is ne–

glected, the solution presented in Figure 4.2 is obtained in 3 iteration steps.

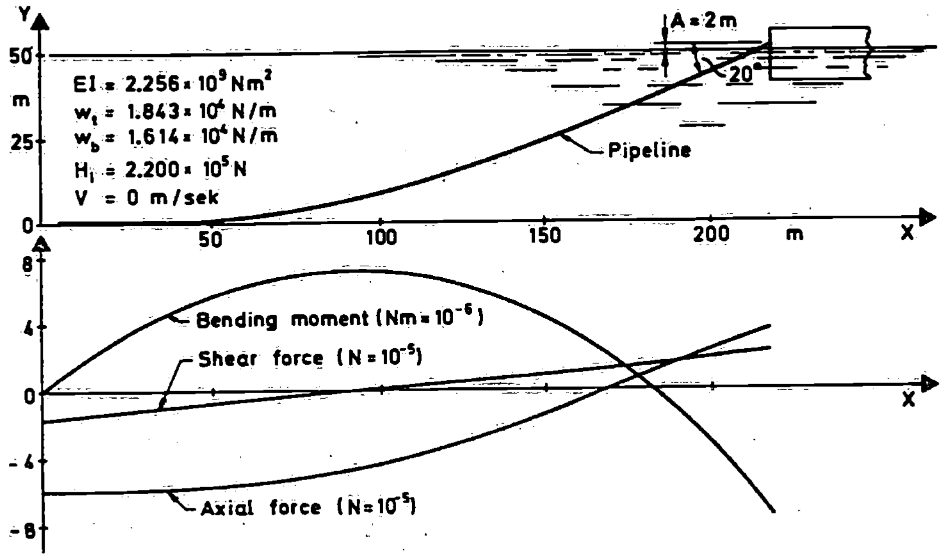

Figure 4.3. Results of numerical analysis of pipe–laying procedure without the use of a stinger.

Fig. 4.4 shows the results of the numerical analysis of a pipe–laying procedure where the pipe is laid with the use of a flexible stinger. The water depth H is 300 m.

Starting with a deflection curve corresponding to the solution of the linearized beam equation, where the effect of the applied horizontal tension H_i is neglected, the solution presented in Fig. 4.4. is obtained in 7 iteration steps.

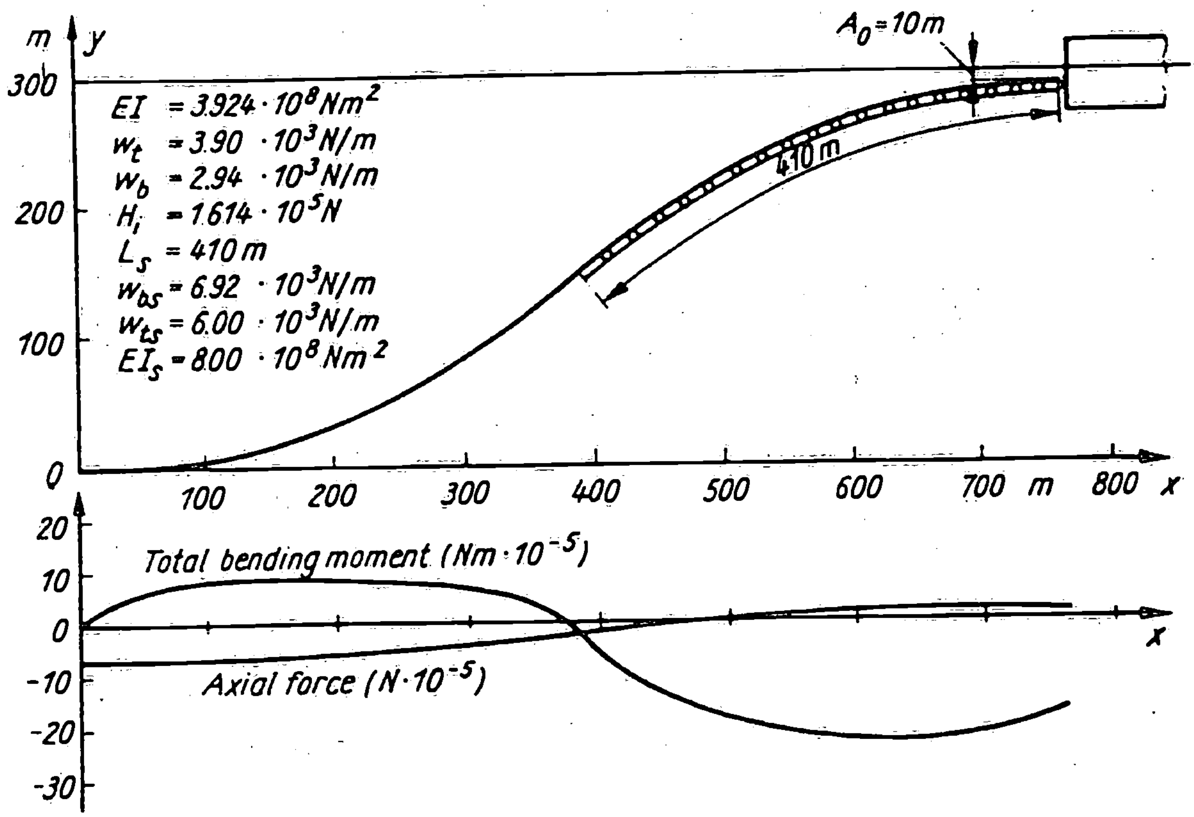

Figure 4.4. Results of numerical analysis of pipelaying using a flexible stinger.

B. Pipe–laying using a rigid stinger

We will now consider pipe–laying with the use of a rigid stinger with a fixed curvature $1/R$ as shown in figure 1.1. Let us assume that the applied horizontal tension is H_i at the upper end of the suspended pipe (the lift–off point from the stinger). The tangent angle of the stinger at the point where the stinger is hinged to the barge is denoted θ_u. The angle θ_u will normally be a non–linear function of the position of the lift–off point given by Y_i and θ_i and the magnitude of the concentrated force T_i perpendicular to the stinger axis at the lift–off point. Due to the constant curvature of the stinger the force T_i equals the shear force in the pipe just below the lift–off point. The functions

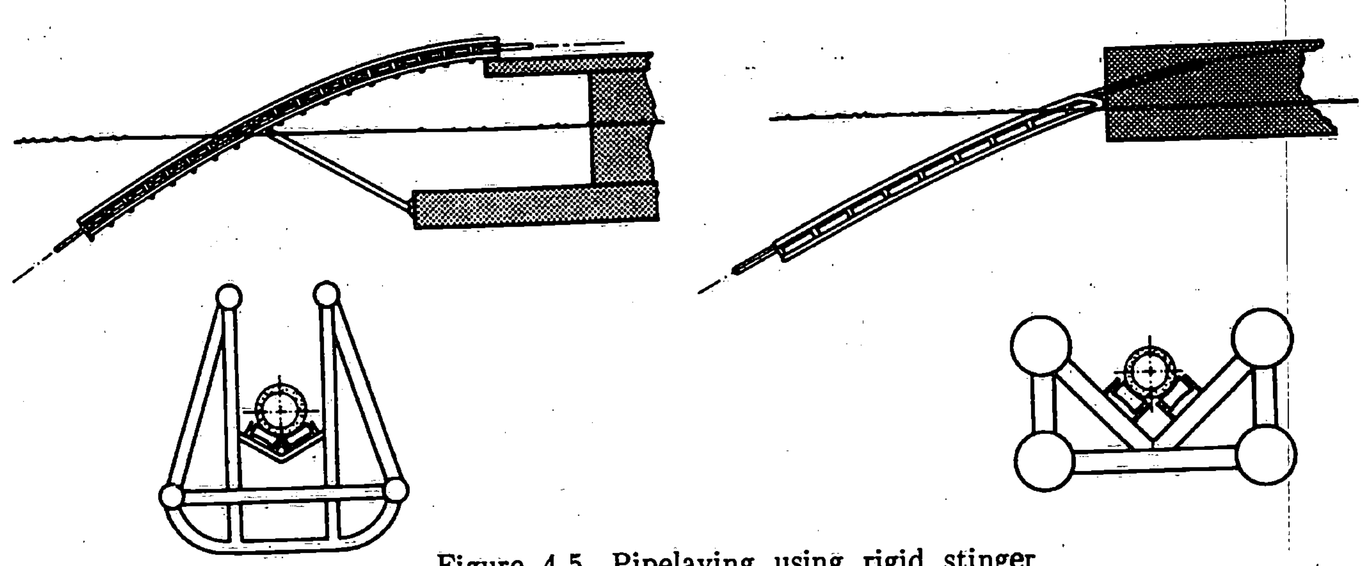

Figure 4.5. Pipelaying using rigid stinger

$\theta_u = \theta_u(Y_i, T_i)$ can be determined when the geometry and the weight distribution of the stinger are known. See figure 4.6.

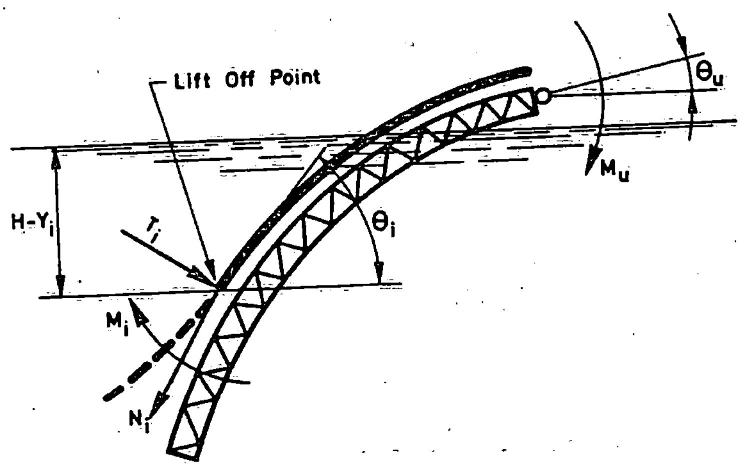

Figure 4.6. The stinger supported part of the pipe.

Besides the static boundary condition expressing the fact that the horizontal force is H_i at the lift–off point then the bending moment M_i is also given

$$M_i = - EI/R \tag{4.8}$$

Finally, kinematic considerations give us the relationship

$$\cos\theta_i = \cos\theta_u - \frac{H - Y_i + A}{R} \tag{4.9}$$

The iteration algorithm for the solution of this problem is similar to the algorithm which was described for the solution of the problem where the angle θ_i was known. Only in this case we know the bending moment at the upper end, Eq. (4.8), therefore we do not need to introduce the auxiliary function $m^{(2)}_{j+1}(\xi)$ in the Eq. (4.4).

The equation used to determine the unknown suspended length λ_{j+1} is derived from a transcendental equation obtained from the boundary condition (4.1a) and Eq. (4.6b):

$$\cos\theta_{j+1}(1) \quad = \cos\theta_u - \frac{1}{r}\left\{1 + a - \lambda_{j+1}\, y_{j+1}(1)\right\} \tag{4.10}$$

The method outlined is, of course, only valid when the stinger is so long that the calculated lift–off point is on the stinger. If this is not the case, a slightly different iteration scheme is called for.

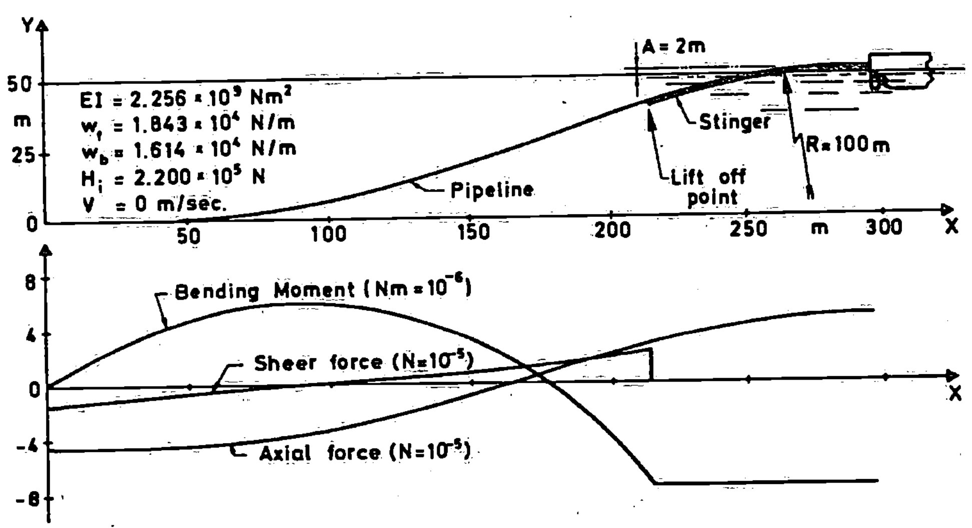

Figure 4.7. Results of numerical analysis of pipe–laying procedure with the use of a rigid stinger.

An example of the numerical analysis of a pipe–laying procedure using a stinger with fixed curvature is shown in figure 4.6. The stinger radius is assumed to be 300 m and in this example, the stinger is assumed to be rigidly connected to the pipe–laying barge. The water depth and the pipe data are assumed to be the same as in the previous example.

C. Pipe abandon/recovery operations

Pipe abandon and recovery operations may be modelled as shown in figure 4.8. These operations can be performed in a number of different ways. As an example we will assume that the wire passes over the stinger rollers and that the horizontal anchor force transmitted to the pipe T_b and the Y–coordinate of the pipe end Y_i are known, whereas the wire tension T_w is considered as a dependent variable.

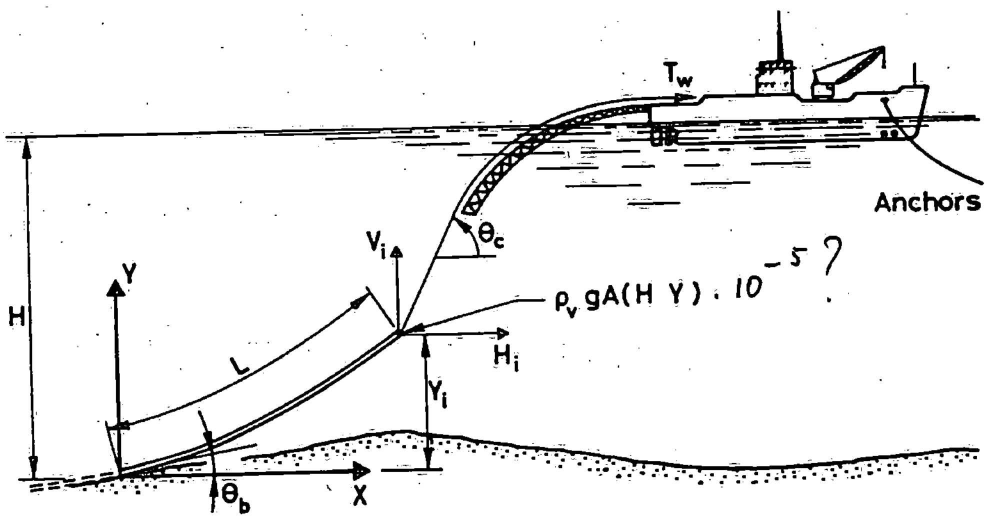

Figure 4.8. Pipe abandon/recovery operation.

Taking into account the water pressure on the lid which is normally welded onto the pipe end during these operations, the boundary conditions for the upper end of the pipe take the form

$$Y(L) = Y_1 \tag{4.11}$$

$$M(L) = 0 \tag{4.12}$$

$$H_i = T_b - w_b(H - Y_i) \cos\theta(L) \tag{4.13}$$

Figure 4.9 shows the results of a numerical analysis of a pipe abandon or recovery operation. The same pipe data as in the previous numerical examples have been assumed. The position of the upper end of the suspended length is specified as 25 m above the ocean floor and the horizontal anchor force as 10^5 N. The necessary wire tension is found to be $2.148 \cdot 10^5$ N.

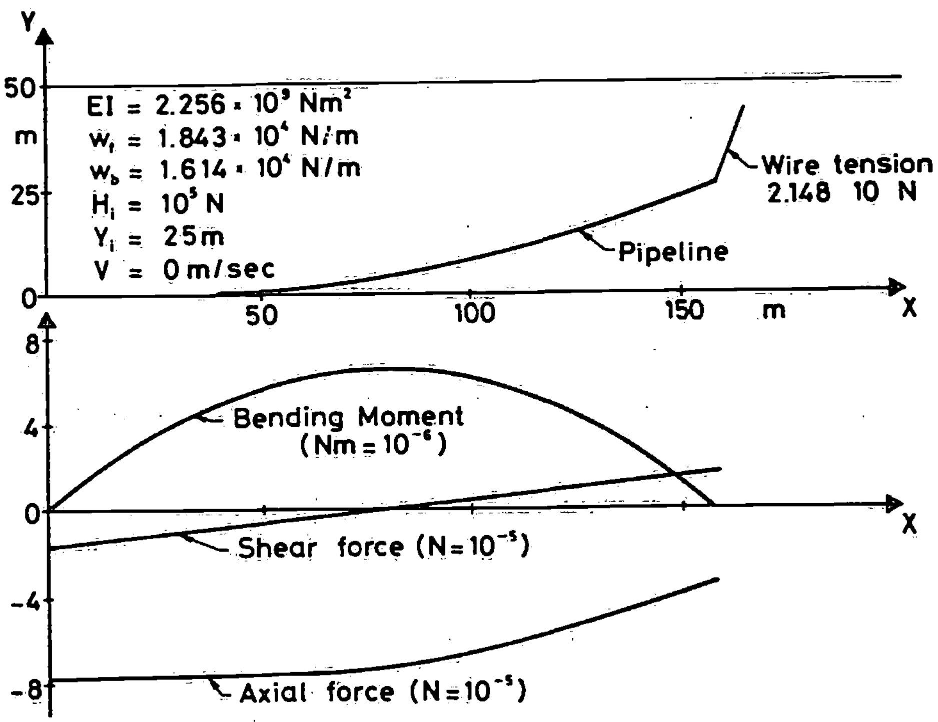

Figure 4.9. Results of numerical analysis of abandon/recovery operation.

5. Conclusion

The method of successive integrations presented for the determination of equilibrium forms and stresses for submarine pipelines during laying possesses several advantages over other available methods. The principal advantage is the extremely modest requirements to computer storage and computer time. Since, in principle, the method only involves integration of known functions, the method is well suited for programming on shipboard computers for control of the actual pipe-laying procedure. Another advantage of the method is its flexibility. For example the effect of variations of pipeline bending stiffness due to variations in the coating, current variations with depth, and auxiliary support buoys can easily be accounted for.

The primary limitation of the present method for the analyses of equilibrium forms of pipes is that in it's presented form it can only deal with 2–D configurations. However, in [15] and [16] it is shown how the procedure can be extended to the 3–D case. Unfortunately, the analysis of 3–D equilibrium forms is considerably more complicated.

6. References

[1] Plunkett, R.: "Static Bending Stresses in Catenaries and Drill Strings", J. of Engineering for Industry Feb. 1967.

[2] Dixon, D.A. and Rutledgde, D.R.: "Stiffened Catenary Calculation in Pipeline Laying Problem", J. of Engineering for Industry Feb. 1968.

[3] Powers, J.T. and Finn, L.D.: "Stress Analysis of Offshore Pipelines During Installation", Offshore Technology Conference, Paper No. 1071, 1969.

[4] Palmer, A.C., Hutchinson, J.W. and Ells, J.W.: "Configuration of Submarine Pipelines During Laying Operations", Trans. of the ASME, J. of Engineering for Industry, Nov. 1974.

[5] Dareing, D.W. and Neathery, R.F.: "Marine Pipeline Analysis Based on Newton's Method with an Arctic Application", J. of Engineering for Industry, Nov. 1970.

[6] Pedersen, P.T.: "Equilibrium of Offshore Calbes and Pipelines During Laying", Int. Shipbuilding Pregress. vol. 22, No. 236, pp. 399 – 408, 1975.

[7] Pedersen, P.T.: "Equilibrium of Marine Pipelines During Laying", Zeitschrift Angewandte Matematik und Mekanek, vol. 58, pp. 228 – 230, 1978.

[8] Gardner, T.N. et al.: "Dynamic Analysis of Risers and Caissons by the Element Method", OTC 2651, 1976.

[9] Chung, J.S. & Felippa, C.A.: "Nonlinear Static Analysis of Deep Ocean Mining Pipe—Part 1, 2", J. of Energy Resources Tech., March 1981, vol 103.

[10] Bernitsas, M.M. et al.: "Large Deformation Three–Dimensional Static Analysis of Deep Water Marine Risers", Applied Ocean Research, vol. 7, No. 4, 1985.

[11] Bryndum, M.B. et al.: "Dynamic Lay Stresses for Pipelines" Offshore Technology Conference, Paper No. 4267, 1982.

[12] Nordgren, R.P.: "On Computation of the Motion of Elastic Rods", J. of Applied Mechanics, Sep. 1974.

[13] Nordgren, R.P.: "Dynamic Analysis of Marine Risers With Vortex Excitation", J. of Energy Resources Technology, March 1982.

[14] Molahy, R.C.: "A Nonlinear Finite Element Method for the Analysis of Offshore Pipelines, Risers and Coth Structures" V^{th} OMAE, Vol.3, pp. 471 – 478, 1986.

[15] Larsen, C.M.: "Static and Dynamic Analysis of Offshore Pipelines During Installation", Norwegian Institute of Technology, Report SK/M35, Trondheim 1976.

[16] Yan, J. & Pedersen, P. Terndrup: " 3–D Static Analysis of Pipelines During Laying". Proc. Offshore Technology Conference, Houston, OTC paper No. 5297, vol 4, pp 47 – 56, 1986.

[17] Yan, J & Petersen, P. Terndrup: "Mathematical Models for Space Curved Pipelines and Risers." Proceedings of the Third Int. Sympo–sium on Practical Design of Ships and Mobile Units, Trondheim, pp. 224 – 236, June 1987.

7. Nomenclature

A	distance between barge deck and water surface
a	cross–sectional area
C_n	normal drag coefficient
C_t	tangential drag coefficient
D	outer diameter of pipe or cable
EI	bending stiffness of pipe
F_n, f_n	normal drag force per unit length
F_t, f_t	tangential drag force per unit length
f_j, g_j	auxiliary functions
H	water depth
H_b, h_b	horizontal force component at the ocean floor
H_i, h_i	horizontal force component at upper end of suspended length
L, λ	suspended length
M, m	bending moment
N, n	axial tension
p_x, p_y p_n, p_t	components of load per unit length
s, ξ	arc length
T	shear force
T_b	horizontal anchor force
V	current velocity
V_b, v_b	vertical force component at ocean floor
V_i, v_i	vertical force component at upper end of suspended length
w_b	buoyancy per unit length
w_t	weight per unit length
X, Y, x, y	rectangular coordinates
θ	tangent angle
ρ_v	mass density of water